

LASERS

PACS numbers: 42.55.Rz; 42.60.Jf; 42.60.Lh
DOI: 10.1070/QE2015v045n01ABEH015644

Investigation of Fe:ZnSe laser in pulsed and repetitively pulsed regimes

S.D. Velikanov, N.A. Zaretskiy, E.A. Zotov, V.I. Kozlovsky, Yu.V. Korostelin, O.N. Krokhin, A.A. Maneshkin, Yu.P. Podmar'kov, S.A. Savinova, Ya.K. Skasyrsky, M.P. Frolov, R.S. Chuvatkin, I.M. Yutkin

Abstract. **The characteristics of a Fe:ZnSe laser pumped by a single-pulse free-running Er:YAG laser and a repetitively pulsed HF laser are presented. An output energy of 4.9 J is achieved in the case of liquid-nitrogen cooling of the Fe^{2+}:ZnSe active laser element longitudinally pumped by an Er:YAG laser with a pulse duration of 1 ms and an energy up to 15 J. The laser efficiency with respect to the absorbed energy is 47%. The output pulse energy at room temperature is 53 mJ. The decrease in the output energy is explained by a strong temperature dependence of the upper laser level lifetime and by pulsed heating of the active element. The temperature dependence of the upper laser level lifetime is used to determine the pump parameters needed to achieve high pulse energies at room temperature. Stable repetitively-pulsed operation of the Fe^{2+}:ZnSe laser at room temperature with an average power of 2.4 W and a maximum pulse energy of 14 mJ is achieved upon pumping by a 1-s train of 100-ns HF laser pulses with a repetition rate of 200 Hz.**

Keywords: *Fe:ZnSe laser, Er:YAG laser, HF laser, solid-state tunable laser, mid-IR laser.*

1. Introduction

Particular interest in lasers emitting at a wavelength close to 4 μm is related to the transparency window of the Earth's atmosphere. For some applications, it is necessary to have pulsed lasers with an energy of several joules, as well as lasers operating in the repetitively pulsed regime. Laser wavelength tunability within the atmospheric transparency window is also important.

S.D. Velikanov, N.A. Zaretskiy, E.A. Zotov, A.A. Maneshkin, R.S. Chuvatkin, I.M. Yutkin Russian Federal Nuclear Centre 'All-Russian Research Institute of Experimental Physics', prosp. Mira 37, 607190 Sarov, Nizhnii Novgorod region, Russia;
e-mail: velikanov@otd13.vniief.ru;
V.I. Kozlovsky, O.N. Krokhin P.N. Lebedev Physics Institute, Russian Academy of Sciences, Leninsky prosp. 53, 119991 Moscow, Russia; National Research Nuclear University 'MEPhI", Kashirskoe sh. 31, 115409 Moscow, Russia; e-mail: vikoz@sci.lebedev.ru;
Yu.V. Korostelin, Ya.K. Skasyrsky P.N. Lebedev Physics Institute, Russian Academy of Sciences, Leninsky prosp. 53, 119991 Moscow, Russia;
Yu.P. Podmar'kov, S.A. Savinova, M.P. Frolov P.N. Lebedev Physics Institute, Russian Academy of Sciences, Leninsky prosp. 53, 119991 Moscow, Russia; Moscow Institute of Physics and Technology (State University), Institutskii per. 9, 141700 Dolgoprudnyi, Moscow region, Russia; e-mail: yupetpo@yandex.ru

Received 24 July 2014; revision received 2 September 2014
Kvantovaya Elektronika **45** (1) 1–7 (2015)
Translated by M.N. Basieva

Several types of lasers of this region are being developed. High-power DF lasers only partially cover the spectral range above 4 μm. It is possible to create repetitively pulsed optical parametric oscillators with a pulse duration of several nanoseconds and an energy up to 0.1 J. However, these oscillators are difficult to align and are insufficiently reliable. The development of semiconductor quantum cascade lasers requires advanced epitaxial technology. In addition, these lasers can hardly be used for producing pulsed sources with a joule-level energy and good beam quality. In this connection, it seems promising to study Fe^{2+}:ZnSe lasers tunable within the range 3.77–5.05 μm [1–3].

Previously [4], it was reported that an output energy of 0.42 J was achieved in a laser based on Fe:ZnSe crystal cooled with liquid nitrogen and pumped by an Er:YAG laser. In [5], we succeeded in increasing the pulse energy to 2.1 J at $T = 85$ K. This was achieved by increasing the pump energy and the size of the active volume in the Fe:ZnSe crystal. The output laser energy was observed to saturate with increasing pump energy due to an unknown reason. The pulse energy decreased with increasing temperature of the crystal, which we related to a strong temperature dependence of the upper laser level lifetime and to pulsed heating of the active element (AE). In particular, the laser pulse energy at room temperature was as low as 42 mJ at a slope efficiency of only 3%.

To increase the laser efficiency at room temperature, it is necessary to use a short pump pulse, shorter than the upper laser level lifetime. In the case of pumping by a giant pulse of a passively Q-switched Er:YAG laser, we obtained pulses with an energy of 6 mJ at a slope efficiency of 39% [6]. Higher energies were achieved upon pumping by more powerful HF laser pulses [7–9]. The highest energy of 192 mJ was achieved at a pulse duration at half maximum of 90 ns [9]. The use of electric discharge HF(DF) lasers for pumping allows one to achieve high energy characteristics. This is explained by a short pulse duration (100–200 ns) and by the possibility of producing repetitively pulsed sources with a sufficiently high output energy [10, 11]. Further increase in the energy is possible by using large-volume active crystals; in this case, it is necessary to minimise the parasitic effect of inversion drop by amplified spontaneous noise, which is typical for high-gain laser media, in particular, for semiconductor lasers [12]. To increase the active length of the crystal, it is necessary to decrease the concentration of Fe ions and the optical gain. For this purpose, the crystals should be made by a technology minimising the concentration of defects responsible for the residual absorption in the crystal. From this viewpoint, growth from the vapour phase with simultaneous doping in the growth process [6, 13] is much more advantageous than

the widely used two-stage technology based on solid-state diffusion of Fe atoms.

An increase in the laser output energy can also be achieved due to pumping by a train of short pulses. Let us consider a case when the train duration is limited by the characteristic heat transfer time t_0 inside the active crystal,

$$t_0 = r^2\rho c/\chi, \quad (1)$$

where r is the characteristic size of the crystal in the direction perpendicular to the cavity axis, while ρ, c and χ are the density, specific heat capacity and thermal conductivity of the crystal. At $r = 0.4$ cm, $\rho = 5.42$ g cm^{-3}, $c = 0.339$ J g^{-1} K^{-1} and $\chi = 0.19$ W cm^{-1} K^{-1}, we obtain $t_0 = 1.5$ s, i.e., the characteristic time of heat transfer from the centre of the crystal with the cross section of 8 × 8 mm to its side surface is 1.5 s. At longer pulse trains, an important role is played by the heat transfer from the crystal to an external heat sink of the AE cooling system. At $t_0 < 1.5$ s, temperature restrictions only slightly depend on the pulse train duration.

In this work, we managed to considerably increase the laser energy in the case of millisecond pump pulses and liquid-nitrogen cooling by increasing the pump energy and suppressing the inversion drop caused by amplified spontaneous noise, as well as to increase the laser energy at room temperature by pumping the crystal by HF laser pulse trains with a duration of ~1 s.

2. Experimental

The active laser elements were cut from Fe:ZnSe single crystals grown on a single crystal seed by chemical vapour transport in hydrogen [13]. Doping with Fe^{2+} ions was performed directly during the growth. The wavelength dependence of the Fe:ZnSe absorption cross section is shown in Fig. 1. The presented absolute absorption cross sections are obtained by normalising to the maximum absorption cross section of 0.97×10^{-18} cm^2 taken from [14].

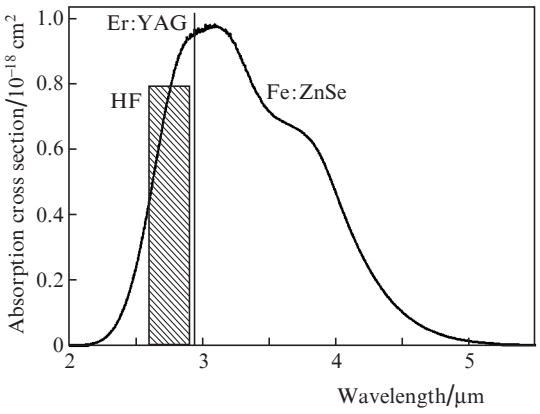

Figure 1. Absorption spectrum of a Fe:ZnSe crystal at room temperature, as well as Er:YAG laser emission line (2.94 μm) and HF laser spectral range (2.6–2.9 μm).

In this work, we studied the laser characteristics of Fe:ZnSe crystals using two different experimental setups. Figure 2 shows the scheme of the experimental setup for investigating a Fe:ZnSe laser (concentration of Fe^{2+} ions

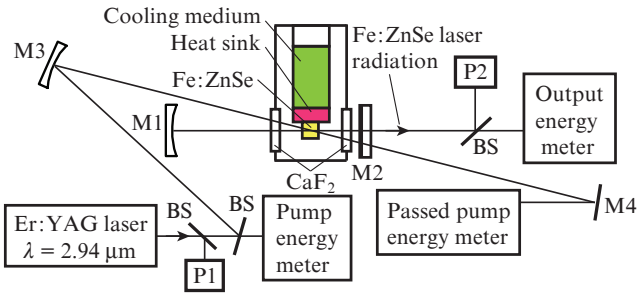

Figure 2. Scheme of the setup with pumping by an Er:YAG laser: (M1)–(M4) mirrors; (P1), (P2) photoresistors; (BS) beam splitters.

2.5×10^{18} cm^{-3}) upon pumping by a free-running Er:YAG laser.

The AE had a form of a parallelepiped with a cross section of 9.7 × 10.1 mm and a length of 7.7 mm (gain length), whose faces were polished but not antireflection coated. The angle between the faces did not exceed 20″. To reduce the inversion drop due to the spontaneous noise propagating in the direction perpendicular to the optical cavity axis, the side surfaces of the crystal were ground and coated (blackened) with aquadag. The AE was fixed on a copper heat sink in an evacuated cryostat cooled with liquid nitrogen. The cryostat windows were made of plane-parallel CaF_2 plates without antireflection coatings. The plates and the crystal faces were perpendicular to the optical cavity axis.

The Fe:ZnSe laser cavity was formed by a highly reflecting spherical mirror M1 with a curvature radius of 1000 mm and a plane semitransparent output coupler M2. The output coupler transmittance at the lasing wavelength was 72%; the cavity length was 350 mm.

As a pump source, we used a pulsed lamp-pumped Er:YAG laser operating in the free-running regime at a wavelength of 2.94 μm. The pulse duration was 950 μs. The pulse consisted of chaotic spikes with durations of 0.3–1 μs. The pulse energy reached 15 J. The Er:YAG laser beam focused into a spot 6 mm in diameter (95% of the energy) fell on the Fe:ZnSe crystal at an angle of 3° to the optical cavity axis. The pump spot area on the AE surface was approximately twice as large as in [5].

Cooling of the Fe:ZnSe crystal leads to narrowing of its absorption line, while the absorption cross section at the wavelength of the Er:YAG laser at the liquid-nitrogen temperature is approximately 20% larger than that at room temperature [15].

Using the second setup, whose scheme is shown in Fig. 3, we studied the operation of a Fe:ZnSe laser (concentration of Fe^{2+} ions 1.9×10^{18} cm^{-3}) pumped by an electric-discharge repetitively pulsed HF laser at room temperature. In this case, the AE had a cross section of 8 × 8 mm and an active length of 8 mm. The angle between the crystal faces was 2.5′.

As a pump source, we used a HF chemical laser. The pulse energy reached 130 mJ at a pulse duration at half maximum of 100 ns. The pulse repetition rate was 100 or 200 Hz. The HF laser spectrum consisted of several lines within the range 2.6–2.9 μm. The transverse dimensions of the pump laser beam were 15 × 18 mm. This beam was focused by a spherical mirror with a focal length of 750 mm on the AE surface into a spot 3.5–3.7 mm in diameter (90% of the energy).

The laser energy was measured using the scheme shown in Fig. 3a. In this case, the Fe:ZnSe laser was pumped through

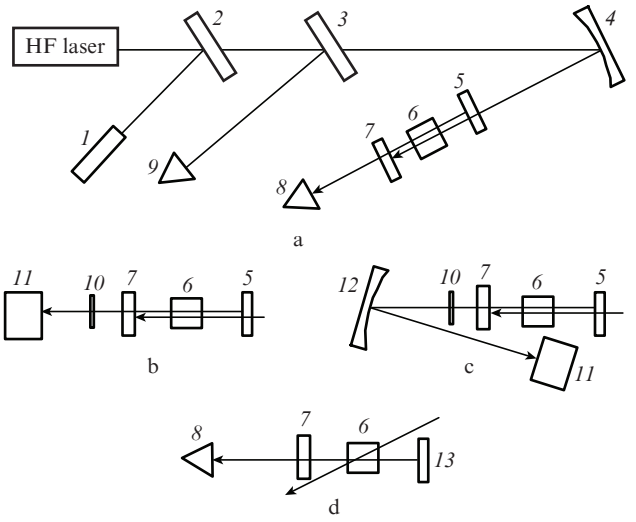

Figure 3. Scheme of the setup with pumping by an HF laser (a), schemes for measuring near- (b) and far-field (c) laser radiation patterns, and scheme for measuring the pulse shape (d): (*1*) alignment laser; (*2*), (*3*) CaF_2 plates; (*4*) spherical mirror with a focal length of 750 mm; (*5*) plane dichroic highly reflecting mirror of the optical cavity; (*6*) Fe^{2+} : ZnSe active element; (*7*) plane output coupler of the optical cavity; (*8*) and (*9*) Coherent J-25MB-HE pyroelectric sensors (for measuring pulse energy) or NFPU 'Orion' photodetectors (for measuring pulse shape); (*10*) germanium filter; (*11*) Pyrocam III camera; (*12*) spherical mirror with a focal length of 1000 mm; (*13*) plane copper mirror.

a plane dichroic mirror (*5*), which, together with a plane mirror (*7*), formed the optical cavity of the Fe : ZnSe laser. The cavity length was 106 mm. The transmittance of mirror *5* at the pump wavelength was 84.2%, while the reflection coefficient at the Fe : ZnSe laser wavelength (4–5 μm) exceeded 99%. The reflection coefficient of the output coupler (*7*) was 80% for the lasing wavelength and 95.8% for the pump radiation. The energy of the Fe : ZnSe and HF laser pulses was measured with Coherent J-25MB-HE pyroelectric sensors. The oscillograms of laser pulses were recorded with NFPU 'Orion' photodetectors.

To record the near- and far-field intensity distributions, we used the schemes fragmentarily shown in Figs 3b and 3c, respectively. The intensity distribution pattern was recorded using a Pyrocam III camera. The far field was formed in the focal plane of a spherical mirror with a focal length of 1000 mm. The scheme shown in Fig. 3d was used to record the temporal profiles of laser pulses at different pump energies. In this case, the pump laser beam was directed to the crystal at an angle of 5°; the cavity length was 178 mm. A copper mirror was used as a highly reflecting mirror.

3. Experimental results

Figure 4 presents the dependence of the Fe : ZnSe laser pulse energy on the absorbed energy of the Er : YAG laser pulse at a temperature of 85 K. For comparison, Fig. 4 also shows the corresponding dependence obtained by us in [5]. We managed to increase the maximum pulse energy to 4.9 J, i.e., approximately by a factor of 2.5. In this case, the laser efficiency with respect to the absorbed energy was ~47%. These results were achieved due to an increase in the transverse dimensions of the active region and to a weaker effect of the inversion drop caused by amplified spontaneous radiation in the transverse direction, which allowed us to increase the pump energy. The

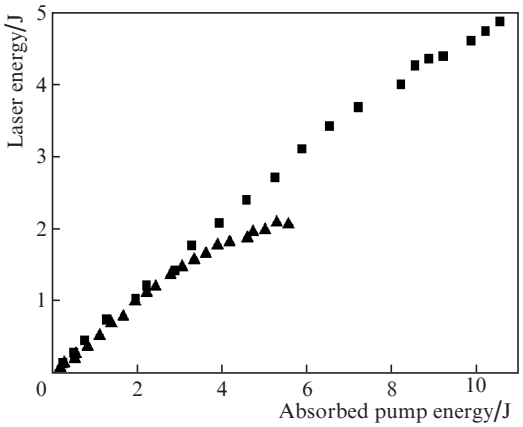

Figure 4. Dependence of the Fe : ZnSe laser pulse energy on the absorbed energy of an Er : YAG laser pulse at $T = 85$ K measured in the present work (squares) and in our previous study [5] (triangles).

maximum energy at $T = 85$ K is limited only by the absorbed pump energy. The lasing threshold was 140 mJ. The laser pulse, as well as the pump pulse, consisted of spikes with a characteristic duration of 0.3–1 μm.

An increase in temperature to $T = 245$ K led to an approximately twofold decrease in the laser efficiency, which allows one to obtain laser energy of 2–3 J when cooling the AE with a thermoelectric Peltier element. However, further increase in temperature leads to a considerable decrease in the pulse energy, because of which we obtained at room temperature only an energy of 53 mJ. This decrease is related to a strong temperature dependence of the upper laser level lifetime and to pulsed heating [5]. The latter caused shortening of the laser pulse with respect to the pump pulse. To increase the laser efficiency at room temperature, one should use a train of short pulses with a duration shorter than the upper laser level lifetime.

Figure 5 shows the dependence of the energy of an individual output pulse of the Fe : ZnSe laser on the absorbed energy of the HF pump laser at room temperature (295 K). The measurements were performed using the scheme shown in Fig. 3a. The maximum energy was 14.4 mJ at an absorbed energy of 58 mJ, the laser efficiency and slope efficiency being

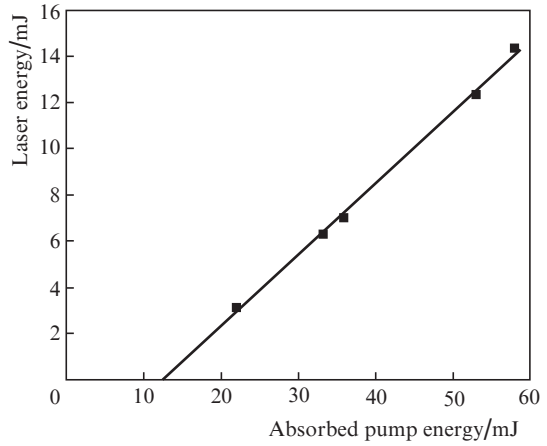

Figure 5. Dependence of the single-pulse energy of a Fe : ZnSe laser on the absorbed energy of a HF laser.

25% and 31.3%, respectively. The lasing threshold estimated by extrapolating the obtained dependence is 13 mJ.

The oscillograms of individual pump and laser pulses are given in Fig. 6 for three different absorbed pump energies. The measurement scheme is shown in Fig. 3d. One can see that the laser pulse contains relaxation spikes. This pulse is delayed with respect to the pump pulse, this delay decreasing with increasing excess over the lasing threshold.

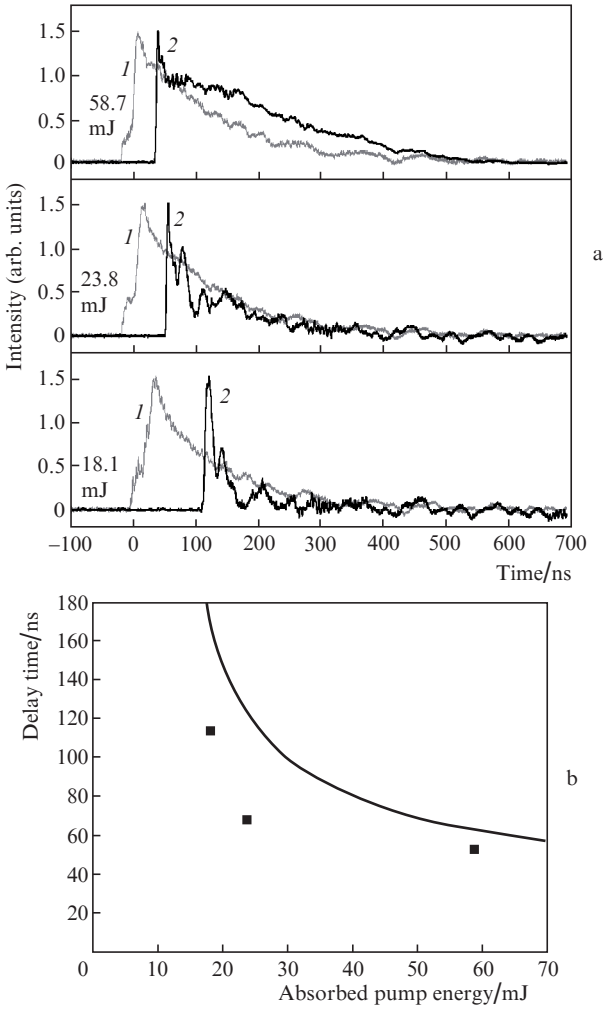

Figure 6. Oscillograms of the pulses of the HF pump laser (*1*) and Fe:ZnSe laser (*2*) at pump pulse energies of 18.1, 23.8, and 58.7 mJ (a), as well as dependence of the laser pulse delay with respect to the pump pulse at a level of 0.1 of the intensity on the absorbed pump energy (b) (the points and the curve correspond to experiment and calculation, respectively).

Figure 7 shows the pulse-to-pulse changes in the laser pulse energy and efficiency in two typical trains with a duration of 1 s and pulse repetition rates of 100 and 200 Hz (see the measurement scheme in Fig. 3a). At a pulse repetition rate of 100 Hz, one sees a high temporal stability of efficiency and energy. Some decrease in these parameters is observed at a pulse repetition rate of 200 Hz, which is related to a slight decrease in the pump energy and to heating of the active element. The average train power was 1.4 and 2.4 W at pulse repetition rates of 100 and 200 Hz, respectively. The total train energies were, respectively, 1.4 and 2.4 J.

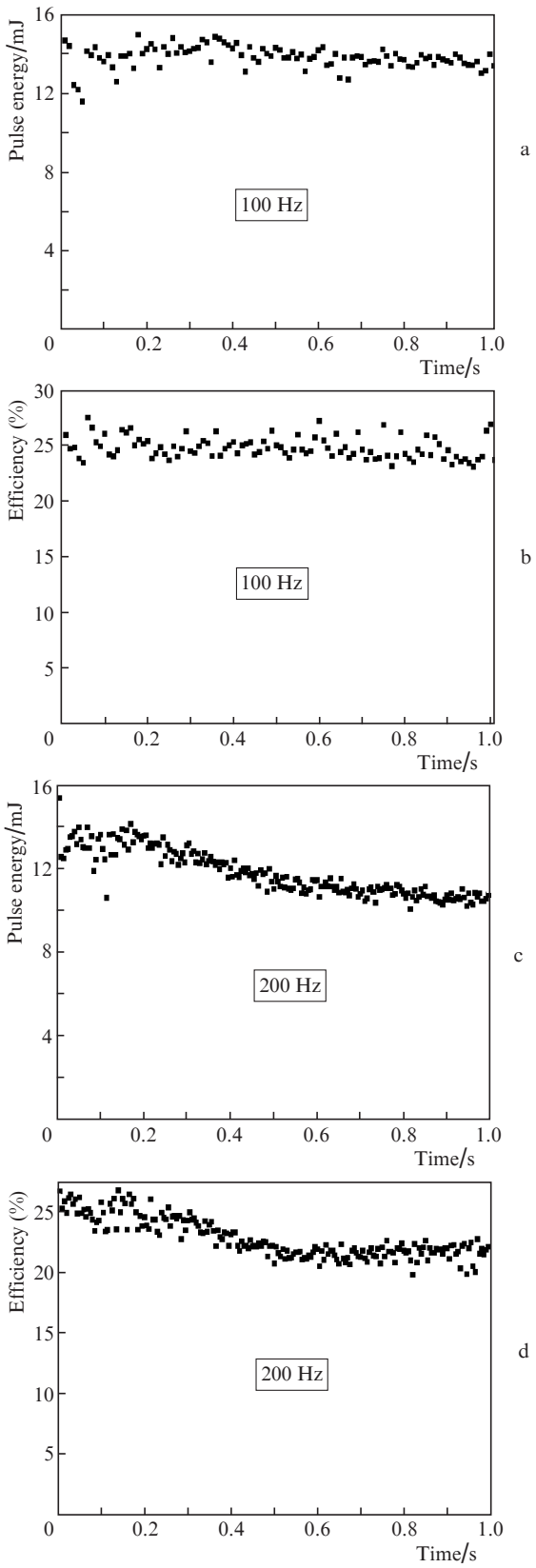

Figure 7. Changes in the laser pulse energy (a, c) and efficiency (b, d) from pulse to pulse (each point is an individual pulse) in 1-s trains with different pulse repetition rates.

Figure 8 presents the near- and far-field patterns of the Fe:ZnSe laser radiation for an individual pulse. The spot size and the total divergence angle at a level of 1/e of the maxi-

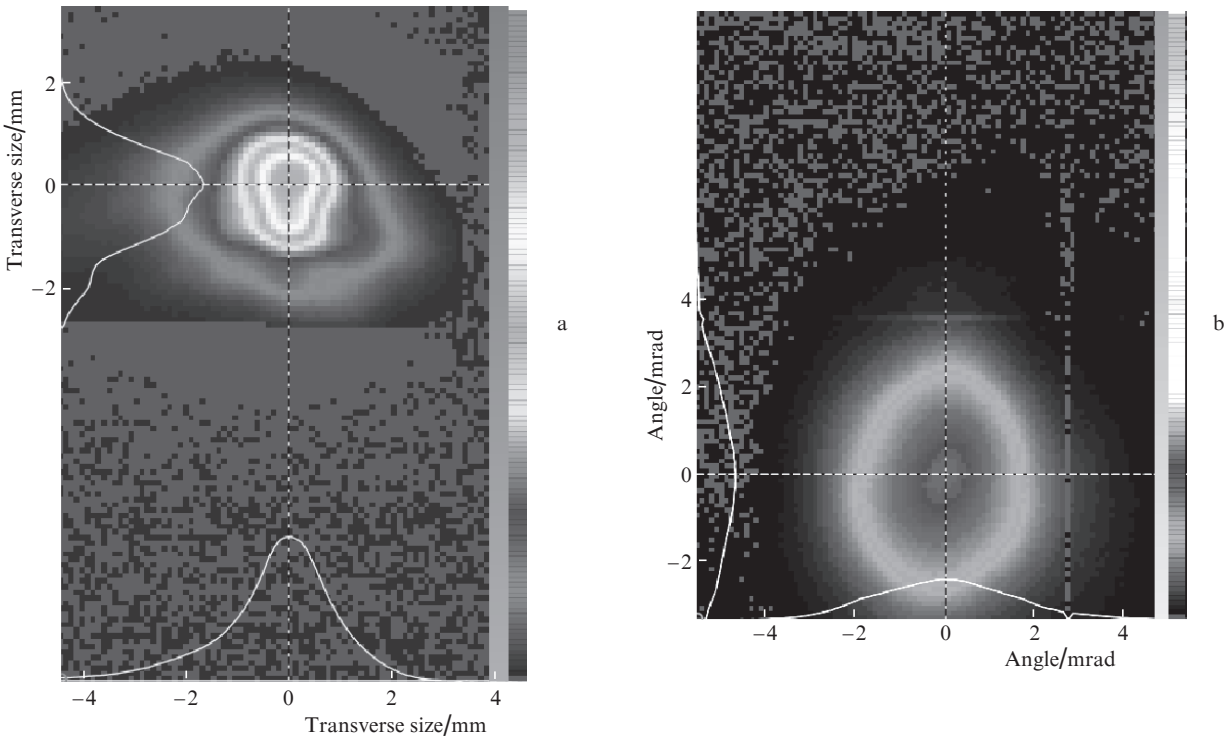

Figure 8. Near- (a) and far-field (b) patterns of the Fe^{2+}:ZnSe laser radiation.

mum intensity were 2.2 mm and 3.8 mrad. This is only twofold larger than the Gaussian beam divergence. The absence of axial symmetry in the near- and far-field patterns of the laser radiation can be causes by the elliptical pump spot and by a too large wedge between the crystal faces.

4. Discussion of results

The deterioration of laser energy characteristics with increasing temperature is related to the temperature dependence of the upper laser level lifetime. This dependence above room temperature was measured in [5]. The upper laser level lifetime for Fe:ZnSe crystals can be represented in the form

$$\frac{1}{\tau} = \frac{1}{\tau_r} + W_{nr}\exp\left(-\frac{E_a}{kT}\right), \qquad (2)$$

where τ_r is the radiative lifetime; and E_a and W_{nr} are the activation energy and the nonradiative recombination rate. In the measured temperature range, the radiative recombination can be neglected and the nonradiative recombination parameters can be determined quite correctly. For Fe:ZnSe crystals, it was found that $E_a = 277$ meV and $W_{nr}^{-1} = 5$ ps.

Moreover, shortening of the Fe:ZnSe laser oscillation time with increasing energy of the Er:YAG laser at room temperature points to a pronounced dependence of the laser pulse energy on dynamic heating of the crystal during one pulse [5]. Indeed, in the case of homogeneous absorption of 10 J in an active volume of 15 cm^3 of the ZnSe crystal with a volumetric heat capacity of 1.88 J cm^{-3} K^{-1}, the temperature increases by 35 K. In reality, pump radiation is inhomogeneous both along the crystal and over its cross section, because of which the maximum increase in the temperature on the frontal face of the crystal will be more significant. Based on the measured temperature dependence of the upper laser level lifetime [formula (2)], at this heating one can expect a further decrease in the upper laser level lifetime and an increase in the lasing threshold during the pump pulse. The pump inhomogeneity along the active crystal can be decreased by using bidirectional pumping or by reflection of unabsorbed pump radiation from the second face of the crystal. However, even in the case of uniform pumping, formula (2) indicates that, if the crystal is thermostated at $T = 295$ K and heated during a pulse by 35 K (to $T = 330$ K), then the upper laser level lifetime to the end of the pulse will be 100 ns.

The lasing threshold in the quasi-steady-state regime is mainly determined by the upper laser level lifetime. As the crystal temperature changes from 85 to 295 K, the lifetime changes from 57 to 0.35 μs, i.e., by a factor of 163. Since the lasing threshold observed in [5] at $T = 85$ K was 70 mJ, the threshold in the quasi-steady-state regime at room temperature (in the beginning of the pulse) must be no lower than 11.4 J. Nevertheless, lasing occurs due to the spike structure of the pump pulse. The duration of the pump spikes (0.3–0.5 μs at maximal energies) is comparable with the upper laser level lifetime in the beginning of the pulse. The peak power in spikes is higher than the pulse-average power. However, lasing ceases in the second half of the pump pulse when the upper laser level lifetime decreases below 100 ns.

Upon pumping by single pulses (100 ns) of a HF laser, we achieved a rather high slope efficiency of 31.3%, though it is lower than 53% achieved at a low crystal temperature. The output energy was 14.4 mJ at an absorbed pump energy of 58 mJ.

The energy absorbed in a 1-s train of 100 pulses was 5.8 J. Taking into account the lower size of the excited region in the case of pumping by a HF laser, we find that the specific absorbed energy is approximately equal to the specific absorbed energy in the case of pumping by an Er:YAG laser. However, the laser energy upon pumping by a train of short

pulses is 26 times higher than the energy that can be achieved in the case of pumping by an Er : YAG laser at room temperature (1.4 J versus 53 mJ). In the present work, the pulse repetition rate in the train did not exceed 200 Hz. At this rate, the crystal absorbed an energy of 11.6 J. This is comparable with 10 J in the case of pumping by an Er : YAG laser. However, during one second, the heat is transferred to the crystal volume exceeding the excitation region, and about 25% of the absorbed energy is spent to radiation. It is estimated that the increase in the crystal temperature does not reach 35 K, and, hence, the upper laser level lifetime will exceed 100 ns to the end of the train of short pulses.

So that the energy absorbed by the crystal for 1 ms was 10 J (similar to the case of pumping by an Er : YAG laser), the HF laser must operate with a repetition rate of 170 kHz. In this case, heating will be stronger and the lifetime shorter. To evaluate the possibility of operating at a high repetition rate of short pulses, we performed numerical simulation of laser operation based on standard balance equations for the density of active particles and photons in the cavity based on the assumption of a four-level lasing scheme. In this model, it is taken into account that the pump intensity decreases along the crystal length and it is assumed that pumping is homogeneous over the active region cross section. The pump pulse shape was taken from experiment. A decrease of the laser energy in the cavity due to the long-wavelength absorption wing of the AE was also taken into account. The absorption cross section at the pump wavelength and the gain cross section at the lasing wavelength were calculated based on the data given in [14].

Figure 9 shows the calculated energy characteristics of the pulsed laser pumped by a HF laser with a pulse duration at half maximum of 100 ns and the temporal pulse shape shown in Fig. 6. Varying the internal losses, we fitted the calculated data to the experimentally measured energy characteristic (Fig. 5) for the upper level lifetime $\tau = 355$ ns at room temperature. In addition, we obtained the same characteristics for smaller values of lifetime. As is seen from Fig. 9, a 30% decrease in the laser energy should be expected for $\tau = 100$ ns and an absorbed energy of 70 mJ. In the case of pumping by a pulse train with a total energy of 10 J and a train duration of 1 ms, the expected increase in the crystal temperature to the end of the train is 35 K, which decreases the upper laser level lifetime from approximately 350 to 100 ns. According to the performed calculations, as a result of this decrease, the individual laser pulse energy at the absorbed pump energy of 58 mJ will decrease from 14.4 mJ in the beginning of the train to 10 mJ at its end. In this case, the train-average laser efficiency is estimated to be 20%. At a pump energy of 10 J, the laser energy can exceed 1 J at room temperature for a pump duration of 1 ms, which considerably differs from pumping by a free-running Er : YAG laser.

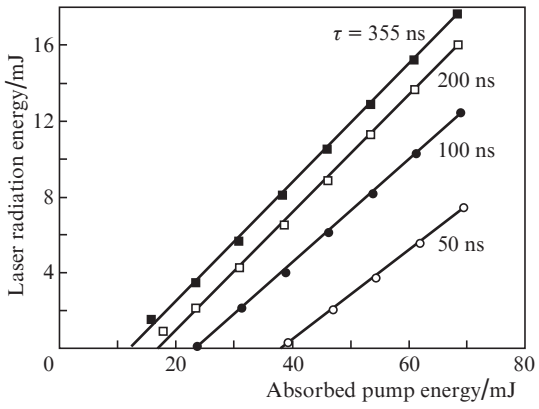

Figure 9. Calculated dependences of the Fe^{2+} : ZnSe laser energy on the absorbed energy of the HF pump laser with a pulse duration at half maximum of 100 ns for different upper laser level lifetimes.

Using numerical simulation, we also calculated the dependence of the laser pulse delay time on the absorbed pump energy (Fig. 6b). The calculated curve and experimental points are in satisfactory agreement.

5. Conclusions

The possibility of producing a pulsed laser based on Fe : ZnSe crystals and operating at a wavelength near 4.1 μm with an energy of 4.9 J at $T = 85$ K is demonstrated. It is shown that a considerable decrease in energy at room temperature is related to a strong temperature dependence of the upper laser level lifetime. To obtain a laser pulse energy of ~1 J at room temperature, it is necessary to use a train of short pulses with a duration shorter than the upper laser level lifetime. When using a repetitively pulsed electric-discharge HF laser with a pulse duration of 100 ns and a pulse energy up to 130 mJ as a pump source, we obtained at room temperature stable repetitively pulsed operation of a Fe : ZnSe laser with an average power of 2.4 W at a pulse repetition rate of 200 Hz, the maximum pulse energy being 14 mJ. The total energy of all pulses for one second was 2.4 J. The energy of 1 J at room temperature can also be obtained for 1 ms by increasing the pulse repetition rate in the train to about 150 kHz.

Acknowledgements. The authors thank I.L. Butsykin, A.F. Zapol'skii and E.A. Saltykov for their help in the work.

References

1. Akimov V.A., Voronov A.A., Kozlovsky V.I., Korostelin Yu.V., Landman A.I., Podmar'kov Yu.P., Frolov M.P. *Kvantovaya Elektron*., **34** (10), 912 (2004) [*Quantum Electron*., **34** (10), 912 (2004)].
2. Fedorov V.V., Mirov S.B., Gallian A., Badikov V.V., Frolov M.P., Korostelin Yu.V., Kozlovsky V.I., Landman A.I., Podmar'kov Yu.P., Akimov V.A., Voronov A.A. *IEEE J. Quantum Electron*., **42**, 907 (2006).
3. Voronov A.A., Kozlovsky V.I., Korostelin Yu.V., Landman A.I., Podmar'kov Yu.P., Skasyrsky Ya.K., Frolov M.P. *Kvantovaya Elektron*., **38** (12), 1113 (2008) [*Quantum Electron*., **38** (12), 1113 (2008)].
4. Mirov S.B. *CLEO Technical Digest* (Washington, OSA, 2012) Paper CM3D.3.
5. Frolov M.P., Korostelin Yu.V., Kozlovsky V.I., Mislavskii V.V., Podmar'kov Yu.P., Savinova S.A., Skasyrsky Ya.K. *Laser Phys. Lett*., **10**, 125001 (2013).
6. Kozlovsky V.I., Akimov V.A., Frolov M.P., Korostelin Yu.V., Landman A.I., Martovitsky V.P., Mislavskii V.V., Podmar'kov Yu.P., Skasyrsky Ya.K., Voronov A.A. *Phys. Stat. Sol. B*, **247**, 1553 (2010).
7. Velikanov S.D., Danilov V.P., Zakharov N.G., Il'ichev N.N., Kazantsev S.Yu., Kalinushkin V.P., Kononov I.G., Nasibov A.S., Studenikin M.I., Pashinin P.P., Firsov K.N., Shapkin P.V., Shchurov V.V. *Kvantovaya Elektron*., **44** (2), 141 (2014) [*Quantum Electron*., **44** (2), 141 (2014)].
8. Gavrishchuk E.M., Kazantsev S.Yu., Kononov I.G., Rodin S.A., Firsov K.N. *Kvantovaya Elektron*., **44** (6), 505 (2014) [*Quantum Electron*., **44** (6), 505 (2014)].

9. Firsov K.N., Gavrishchuk E.M., Kazantsev S.Yu., Kononov I.G., Rodin S.A. *Laser Phys. Lett*., **11**, 085001 (2014).
10. Velikanov S.D., Garanin S.G., Domazhirov A.P., Efanov E.M., Efanov M.V., Kazantsev S.Yu., Kodola B.E., Komarov Yu.N., Kononov I.G., Podlesnykh S.V., Sivachev A.A., Firsov K.N., Shchurov V.V., Yarin P.M. *Kvantovaya Elektron*., **40** (5), 393 (2010) [*Quantum Electron*., **40** (5), 393 (2010)].
11. Butsykin I.L., Velikanov S.D., Evdokimov P.A., Zapol'skii A.F., Kovalev E.V., Kodola B.E., Pegoev I.N. *Kvantovaya Elektron*., **31** (11), 957 (2001) [*Quantum Electron*., **31** (11), 957 (2001)].
12. Bogdankevich O.V., Zverev M.M., Darznek S.A., Ushakhin V.A. *Kvantovaya Elektron*., **2** (8), 1757 (1975) [*Sov. J. Quantum Electron*., **5** (8), 953 (1975)].
13. Akimov V.A., Frolov M.P., Korostelin Yu.V., Kozlovsky V.I., Landman A.I., Podmar'kov Yu.P., Voronov A.A. *Phys. Stat. Sol. C*, **3**, 1213 (2006).
14. Myoung N., Fedorov V.V., Mirov S.B., Wenger L.E. *J. Luminescence*, **132**, 600 (2012).
15. Adams J.J. *New Crystalline Materials for Nonlinear Frequency Conversion, Electro-Optic Modulation, and Mid-infrared Gain Media. PhD Theses* (LLNL, 2002).